MINISTRY OF SUPPLY

AERONAUTICAL RESEARCH COUNCIL
REPORTS AND MEMORANDA

Observations of the Flow Round a Two-dimensional Aerofoil Oscillating in a High-speed Air Stream

By

A. CHINNECK, B.Sc., D. W. HOLDER, Ph.D., and C. J. BERRY,
of the Aerodynamics Division, N.P.L.

LONDON : HER MAJESTY'S STATIONERY OFFICE
1955
FIVE SHILLINGS NET

Observations of the Flow Round a Two-dimensional Aerofoil Oscillating in a High-speed Air Stream

By

A. CHINNECK, B.Sc., D. W. HOLDER, Ph.D., and C. J. BERRY,
of the Aerodynamics Division, N.P.L.

Summary.—Photographs have been taken of the flow round a 10 per cent thick RAE 104 aerofoil performing pitching oscillations at low values of the frequency parameter ($\omega < 0\cdot1$) in subsonic and supersonic air streams. Apart from a difference of phase, the general flow patterns appeared to be similar to those observed in steady motion, the pattern for a particular instantaneous incidence of the oscillation resembling that for steady motion at a different incidence. It is suggested that, for the range of frequency parameter covered, the observed phase lag of the flow pattern corresponds to the lag in the circulation.

The phase lag of the flow pattern (as indicated in most cases by the positions of the regions where transition from laminar to turbulent flow occurs in the boundary layer) has been determined for various conditions of frequency, amplitude and Mach number, and for two positions of the axis of oscillation. For one axis position direct measurements of the pitching-moment derivatives had been made previously, and the phase lag of the flow pattern found in the present experiment is approximately the same as that in the pitching moment.

At the supersonic speed ($M = 1\cdot6$) used in the present tests any phase difference that was present was too small to be detected in a photograph.

---

1. *Introduction.*—Measurements of the pitching-moment damping and stiffness derivative coefficients, $- m_{\dot\theta}$ and m_{θ}, for a 10 per cent thick two-dimensional RAE 104 aerofoil performing pitching oscillations about an axis at $0\cdot445$ chord in a subsonic air stream have been made[1] in the National Physical Laboratory $9\frac{1}{2}$-in. $\times$ $9\frac{1}{2}$-in. Wind Tunnel by Bratt, Raymer and Townsend. The variation with Mach number of these coefficients was considerable, as is shown in Figs. 1 and 2 for several values of the amplitude and frequency of oscillation. In view of these large changes, it seemed desirable to take photographs of the flow pattern round the oscillating aerofoil. This was not possible in the $9\frac{1}{2}$-in. $\times$ $9\frac{1}{2}$-in. tunnel because of the presence of the large frictionless bearings used for supporting the model, and it was decided to make further tests in the 9-in. $\times$ 3-in. tunnel in which a similar aerofoil was oscillated inexorably with an apparatus which obscured a minimum of the optical field.

The present report describes the technique used for flow photography, and the results obtained. The work included not only a direct comparison with the derivative measurements, but also tests at a supersonic speed and with a second model having a different axis position (at $0\cdot195$ chord).

Although the original object of the experiment was solely to reveal the general nature of the flow pattern, it was found during the course of the work that a rough quantitative analysis was possible of the phase differences revealed by the photographs. The accuracy of this analysis (*see* section 5) is not claimed to be high, and is certainly much lower than that which can be achieved in direct measurements of the pitching-moment derivatives.

2. *Description of the Model Aerofoils and the Forcing Apparatus.*—The model aerofoils (Fig. 3) had a RAE 104 section with a span of 3 in., a chord of 2 in., and a thickness/chord ratio of 10

A

per cent. Each model was supported in the tunnel as shown in Fig. 4 by steel rods of 0·2-in. diameter which passed through phosphor-bronze bushes cemented into the glass side walls. For one model the position of the supporting rods was such that the axis of oscillation was 0·445 chord behind the leading edge ; for the other model the axis was at 0·195 chord.

The forcing apparatus is sketched diagrammatically in Fig. 4. A vertical arm, keyed at its lower end to one of the supporting rods, was forked at the upper end ; the inner faces of the fork were in contact with an eccentric driven by the electric forcing motor. The frequency of oscillation was adjusted by varying the speed of the motor by means of a Ward-Leonard system. A similar eccentric and fork (not shown in Fig. 4) were fitted symmetrically to the driving shaft in order to reduce the out-of-balance loads.

Four pairs of eccentrics were provided giving amplitudes of 1, 2, 3 and 4 degrees respectively for the oscillation of the aerofoil. The mean incidence was adjusted by moving the motor mounting parallel to the axis of the tunnel, the movement being measured by a micrometer. The model was set to aerodynamic zero incidence by adjusting the incidence until the flow pattern was symmetrical. This could be done with an accuracy of about $\pm$ 0·1 degree.

The Reynolds number (about $0·8 \times 10^6$ on chord) was the same as for the derivative measurements[1] made previously in the $9\frac{1}{2}$-in. $\times$ $9\frac{1}{2}$-in. tunnel.

3. *Description of the Trigger Circuits used with the Spark Light Sources.*—Direct-shadow photographs of the flow patterns round the aerofoils were taken using a spherical mirror to produce a parallel beam of light, and an electric spark in air to give exposures of the order of one microsecond. The energy in the spark was supplied by a condenser charged by a power pack having an output of 8kV. The spark was triggered at the required point in the forcing cycle by means of a contact in the periphery of a Perspex disc fitted to the shaft of the forcing motor. By moving the contact round the periphery, a series of photographs was obtained throughout the cycle. During the course of the experiment two different circuits were used to trigger the spark.

In the earlier tests at low frequency of oscillation, the spark gap was fitted with a third electrode to form, with one of the main electrodes, an auxiliary gap. This gap was operated from a thyratron-controlled induction coil, and was used to initiate the main discharge. The peripheral contact was connected in series with a manually-operated micro-switch so that closure of the contact after operation of the micro-switch connected the grid of the thyratron to its cathode and triggered the auxiliary gap. Since the charging time of the reservoir condenser in the power pack was several seconds, it was possible to open the micro-switch before a second discharge of the main gap occurred.

The delay between making the peripheral contact and the main discharge was about 200 microseconds. For a frequency of oscillation of 12 c.p.s. this was equivalent to an angular rotation of the forcing shaft of 1 deg, an amount which was found (*see* section 5) to lie within the inherent errors of the experiment. At higher frequencies, however, this angular rotation could no longer be ignored, and the modified circuit shown in Fig. 5 was developed. The new circuit gave a delay of only 20 microseconds which represented an angular rotation of about $\frac{1}{2}$ deg when the frequency was 60 c.p.s.

4. *The Analysis of the Photographs.*—A direct-shadow photograph may frequently be used to determine[2] the state of the boundary layer on the surface of an aerofoil, and the position of the region in which transition from laminar to turbulent flow takes place. The image of a boundary layer contains a bright line running parallel to the shadow of the aerofoil ; when the layer is laminar this line is separated from the surface, but when it is turbulent the line is adjacent to the surface. The transition region occurs as shown in Fig. 6 where the ' laminar line ' bends in towards the ' turbulent line.'

2

Preliminary comparisons of the photographs showed that, at a particular angle of incidence, the general nature of the flow pattern when the aerofoil was oscillating did not differ from that when the aerofoil was stationary. It was clear, however, that in the oscillatory case the movement of the flow pattern lagged behind the movement of the aerofoil. This is illustrated in Fig. 6. The lag could be observed in the motion of the stagnation region near the leading edge, the separation points and the transition regions, as well as in the changes of shock-wave pattern. Of these criteria, only the movements of the transition regions could be determined with reasonable accuracy at Mach numbers below 0·86 because the shock-wave pattern was not sufficiently well defined to enable a particular shock to be followed throughout the cycle. At Mach numbers above 0·86 a high-frequency oscillation similar to that reported[3] by Holder and North masked the effects arising from the oscillation. When the boundary layer was made turbulent (*see* section 7(iii)) from points well forward on the aerofoil, the high-frequency oscillation was suppressed and the shock-waves became more clearly defined.

Unless otherwise stated, the movements of the transition regions have been used in the analysis described below and it is assumed that the results represent also the phase lag in the other features of the flow pattern*. The main justification for this assumption is that comparisons made in a number of cases showed that the phase lags in the movement of the transition regions were of the same order as those in the separation points and in the shock-wave pattern.

Photographs were taken with the aerofoil at incidences corresponding to 0, $\pm\frac{1}{4}\theta_0$, $\pm\frac{1}{2}\theta_0$, $\pm\frac{3}{4}\theta_0$, $\pm\theta_0$, where θ_0 is the amplitude of oscillation. The positions of the transition regions and the incidence of the aerofoil† were measured from each photograph and were plotted against the corresponding angle of the forcing cycle. The optimum sine curves were calculated by the least-squares method, and hence the differences in phase between the motions of the aerofoil and transition regions were found. When transition was fixed artificially near the leading edge (*see* section 7(iii)) the positions of the feet of the shock-waves were used in the analysis.

Curves illustrating the movement of the transition regions when the aerofoil is oscillating at 60 c.p.s. ($\omega = 0\cdot074$) are reproduced in Fig. 7. Curves of the movement of transition for the aerofoil in steady motion ($\omega = 0$) are included to show the phase differences. The scatter of the observed points round the best sine curves is typical, and it should be remembered that a change of $0\cdot01$ in (x_T/c) corresponds to a transition movement of only $0\cdot02$ in. on the surface of the aerofoil.

Altogether about 1,000 photographs were taken during the experiment, and a selection only is reproduced here‡.

5. *The Accuracy of the Analysis.*—If the position of the transition region, x_T/c, found by the above procedure is given by

$$\frac{x_T}{c} = \left(\frac{x_T}{c}\right)_0 \sin\left(\varphi + \varepsilon\right) + \left(\frac{x_T}{c}\right)_s$$

where $(x_T/c)_0$ is the amplitude of movement of the transition region and $(x_T/c)_s$ is the static

---

* Thus, when reference is made to the phase lag in the flow pattern, it is to be understood in most cases that the values quoted are based on measurements of the positions of the transition regions.

† A spike about $\frac{1}{10}$-in. long and $\frac{1}{100}$-in. in diameter was attached to the leading edge of the aerofoil to enable the position of the chord line to be determined with reasonable accuracy from the photographs. The incidence was measured with respect to a datum line which was fixed relative to the tunnel and included in each photograph. The datum line has been omitted from the prints reproduced in the present report.

‡ A Kodak 16-mm high-speed camera was used at 3,000 frames/sec to provide a dynamic record of some of the more interesting cases.

position of the transition region at mean incidence, then the least-squares analysis gives

$$\tan \varepsilon = \frac{B}{A}$$

where

$$A \equiv \frac{\sum\limits_{r=1}^{16} \left\{ \left(\dfrac{x_T}{c} \right)_r \sin \phi_r \right\}}{\sum\limits_{r=1}^{16} \sin^2 \phi_r} \ ,$$

and

$$B \equiv \frac{\sum\limits_{r=1}^{16} \left\{ \left(\dfrac{x_T}{c} \right)_r \cos \phi_r \right\}}{\sum\limits_{r=1}^{16} \cos^2 \phi_r} \ ,$$

and $\sin \phi_r = 0, \ \tfrac{1}{4}, \ \tfrac{1}{2}, \ \tfrac{3}{4}, \ 1, \ \text{———}, \ \tfrac{1}{4}, \ 0, \ -\tfrac{1}{4}, \ \text{———}, \ -1, \ \text{———}, \ -\tfrac{1}{4}.$

$r = 1, 2, 3, 4, 5, \ \text{———}, \ 8, 9, \quad 10, \text{———}, \quad 13, \text{———}, \quad 16.$

The probable errors, E, in A and B (Ref. 4) are given by

$$E_A = \left\{ \sum\limits_{r=1}^{16} \sin^2 \phi_r \right\}^{-1/2} . \ q = 0 \cdot 426 \, q$$

and

$$E_B = \left\{ \sum\limits_{r=1}^{16} \cos^2 \phi_r \right\}^{-1/2} . \ q = 0 \cdot 309 \, q$$

where q is the probable error in reading each of the values $(x_T/c)_r$.

Now since $\tan \varepsilon = B/A$

$$d\varepsilon = \frac{A \ dB - B \ dA}{A^2 + B^2}$$

If we take $dA = E_A$ and $dB = E_B$
then

$$A \ dB - B \ dA = AE_B - BE_A$$
$$= (0 \cdot 309 A - 0 \cdot 426 B)q.$$

If E_ε is the probable error in ε, then [4]

$$E_\varepsilon = \frac{\{(0 \cdot 309 A)^2 + (0 \cdot 426 B)^2\}^{1/2}}{A^2 + B^2} \ . \ q \ .$$

If the value of q is taken as $\pm 0 \cdot 005$, the probable errors in the measured phase differences are of the order ± 1 deg.

6. *Calculation of the Phase Difference from the Pitching Moment Derivatives.*—The aerodynamic pitching moment M_0, per unit span may be written

$$M_0 = M_\theta \theta + M_{\dot\theta} \dot\theta$$

4

where θ is the angle of incidence, and M_θ, $M_{\dot\theta}$ are the derivative coefficients. If θ is given by

$$\theta = \alpha_0 + \theta_0 \sin 2\pi ft$$

M_0 can be expressed in the form

$$M_0 = M_\theta \alpha_0 + \{M_\theta^2 + (2\pi f M_{\dot\theta})^2\}^{1/2}\,\theta_0 \sin(2\pi ft + \eta) \qquad .. \qquad .. \qquad .. \qquad (1)$$

where

$\qquad \alpha_0 \equiv$ mean incidence of oscillation

$\qquad \theta_0 \equiv$ amplitude of oscillation

$\qquad f \equiv$ frequency of oscillation

and

$$\tan \eta = \frac{2\pi f M_{\dot\theta}}{M_\theta} \,.$$

Introducing the non-dimensional forms of the derivative coefficients

$$m_\theta \equiv \frac{M_\theta}{\rho V^2 c^2}$$

$$m_{\dot\theta} \equiv \frac{M_{\dot\theta}}{\rho V c^3}$$

and the frequency parameter, ω, defined by

$$\omega \equiv \frac{2\pi fc}{V}$$

where

$\qquad c \equiv$ chord of aerofoil

$\qquad V \equiv$ velocity of the free stream

$\qquad \rho \equiv$ density of the free stream

we have

$$\tan \eta = \frac{\omega m_{\dot\theta}}{m_\theta} \,. \qquad .. \qquad .. \qquad .. \qquad .. \qquad .. \qquad .. \qquad .. \qquad .. \qquad .. \qquad (2)$$

From equation (1) it is clear that η is the phase difference between the forcing motion and the pitching moment. It follows from equation (2) that positive damping (*i.e.*, negative values of $m_{\dot\theta}$) corresponds to a lag of the pitching moment behind the forcing motion for the rearward axis position ($0 \cdot 445c$), and a lead for the forward axis position ($0 \cdot 195c$), which is in front of the aerodynamic centre.

7. *Discussion of the Results.*—(a) *Tests at Subsonic Speeds.*—(i) *Effects of frequency parameter and axis position* ($\alpha_0 = 0\ deg$, $\theta_0 = 2\ deg$).—The variation of phase lag with Mach number when the axis is at $0 \cdot 445c$ is shown in Fig. 8 for two frequencies, 12 c.p.s. and 60 c.p.s. Also shown in Fig. 8 are curves of the phase lag of the pitching moment calculated from Ref. 1, and curves of the frequency parameter ω. The probable extent of the inaccuracy (*see* section 5) of the points obtained from the photographs is indicated by lines parallel to the ordinate axis. It is seen from Fig. 8 that, at any given Mach number, the phase lag of the flow pattern is approximately proportional to the frequency parameter, and is in reasonable agreement with the phase lag of the pitching moment.

5

The results for a frequency of 60 c.p.s. and with the axis at $0\cdot195c$ are shown in Fig. 9. It is seen from Fig. 9 that the phase lag of the flow pattern is not altered appreciably by the change of axis position.

In order to obtain an indication of the physical significance of the phase lag of the flow pattern, the theoretical lags of the circulation, lift and pitching moment for a flat plate in incompressible flow have been calculated by the methods of Refs. 5 and 6, and the results are plotted in Fig. 10 against frequency parameter. Values for a larger frequency parameter ($\omega = 1\cdot0$) are given in Table 1 for comparison.

TABLE 1

Calculated Phase Lag for a Flat Plate in Incompressible Flow

Frequency parameter ω	Axis at $0\cdot445c$			Axis at $0\cdot195c$		
	Phase lag (degrees) in :			Phase lag (degrees) in :		
	Circulation	Moment	Lift	Circulation	Moment	Lift
0·1	9·2	8·8	4·9	7·6	−10·7	3·5
0·2	13·5	13·3	4·9	10·7	−27·1	2·0
1·0	16·4	27·6	−24·1	4·3	−23·6	−37·6

Fig. 10 shows that for low values of the frequency parameter the calculated lag of the circulation does not change greatly when the axis is altered, and is in good agreement with the calculated lag of the pitching moment for the rearward axis. Since this behaviour is also characteristic of the observed lag of the flow pattern, it is concluded that this lag approximates closely to the lag of the circulation. Table 1 suggests that the close agreement found between the lags of the flow pattern and of the pitching moment for the rearward axis occurs because the frequency parameter of the experiment was low, and would not exist at higher frequency parameters.

W. P. Jones has obtained[7] values (which include an allowance for tunnel-wall interference) for the lags of the circulation and pitching moment with the rearward axis position, by introducing into the unsteady-flow theory the experimental values of the pitching moment and lift-curve slope for steady flow. His results for two values of the frequency parameter are shown in Fig. 11, and values from the curves for the case $\omega = 0\cdot08$ are plotted in Fig. 8. Again it is seen that there is little difference between the calculated moment and circulation for this axis position, and that both these quantities are in reasonable agreement with the phase lag observed in the present tests.

(ii) *The effects of the amplitude of oscillation* ($\alpha_0 = 0$ *deg*, $\theta_0 = 4$ *deg, axis at* $0\cdot445c$).—At an amplitude of 4 deg, the movement of the transition region on the upper surface was no longer linear with incidence throughout the whole cycle, and the variation of transition position with forcing angle was, therefore, no longer sinusoidal. The variation with incidence of the lower-surface transition region remained linear during a half cycle, however, and it was decided to use these values only in the analysis*. The phase lags in the flow pattern for a frequency of 36 c.p.s.† obtained by this procedure are plotted in Fig. 12 where they are compared with values for an amplitude of 2 deg, and with the curve of phase lag in the pitching moment. Since it has been established (*see* section 7(i)) that for 2 deg amplitude the phase lag was proportional to the frequency parameter, no observations were made at 36 c.p.s. for this amplitude and the values plotted in Fig. 12 have been derived from the observations made at 12 c.p.s. and 60 c.p.s. (Fig. 8).

---

* The formulae given in section 5 had to be modified, but the order of the probable error remained unchanged.

† Because of stress limitations in the apparatus, this was the highest frequency used at 4 deg amplitude in the measurements described in Ref. 1.

It appears from Fig. 12 that there is again reasonable agreement between the phase lag of the flow pattern and that of the pitching moment. Also, it is seen that the amplitude has little effect on the phase lag of the flow pattern.

(iii) *The effects of fixing boundary-layer transition* ($\alpha_0 = 0$ *deg*, $\theta_0 = 2$ *deg, axis at* $0 \cdot 445c$).— As mentioned in section 4, the occurrence of a high-frequency oscillation* prevented readings being taken at Mach numbers above $0 \cdot 86$ when the boundary layer was laminar over most of the surface. In order to obtain results at higher Mach numbers it was decided to suppress this oscillation by fixing transition to turbulent flow close to the leading edge of the aerofoil. Transition was fixed at $0 \cdot 2c$ on both surfaces by spoilers about $0 \cdot 005$-in. high, and photographs were taken at Mach numbers of $0 \cdot 86$, $0 \cdot 88$ and $0 \cdot 89$. Since transition was fixed, it was necessary to base the analysis on the positions of the shock-waves. At $M = 0 \cdot 86$ the movement of the shock-waves with changes of incidence was very small, and a detailed analysis was impossible. Examination of the photographs† showed, however, that there was a phase lag which was estimated to be between 15 deg and 20 deg, a value which is somewhat greater than that observed when transition was free (*see* Fig. 8).

At $M = 0 \cdot 88$ and $M = 0 \cdot 89$ the shock-wave movement (Fig. 13) was sufficiently large for measurements to be made with reasonable accuracy, and the derived phase lags are plotted in Fig. 8. It is seen that there is reasonable agreement with the phase lags of the pitching moment derived from measurements[1] made with transition free.

(b) *Tests at a Supersonic Speed* ($\alpha_0 = 0$ *deg*, $\theta_0 = 2$ *deg, Axis at* $0 \cdot 445c$).—Photographs were taken for a Mach number of $1 \cdot 6$ and frequencies of 30 c.p.s. and 60 c.p.s. It was found that the phase difference was too small to be detected ; this may be seen from Fig. 14 which shows the aerofoil at zero incidence whilst static and whilst oscillating at 30 c.p.s. and 60 c.p.s. This result was anticipated because the measurements of the pitching-moment derivatives at supersonic speeds reported[8] by Bratt and Chinneck suggested that the phase lag at 60 c.p.s. would be only about 5 deg. This lag corresponds to a change in the inclination of the shock wave at the trailing edge of the aerofoil of $\frac{1}{4}$ deg, which lies within the margin of error to be expected in measuring the angle of a shock-wave from a direct-shadow photograph.

8. *Previous Photography of the Flow round an Oscillating Aerofoil.*—Apart from some work at very low air speeds (of the order of 20 ft/sec), the only other photographs known to the authors of the flow round an oscillating aerofoil are those taken with an interferometer at Volkenrode. In the tests reported[9] by Zobel, the pressure distribution on an aerofoil of $0 \cdot 07$ metre ($2 \cdot 75$ in.) chord was measured whilst the aerofoil was performing pitching oscillations in an air stream of Mach number $0 \cdot 3$. The method was subsequently extended[10] by Ritter to an aerofoil of $0 \cdot 10$ metre ($3 \cdot 95$ in.) chord with and without a trailing-edge flap. The frequency parameter was about $0 \cdot 2$ for the smaller aerofoil, and $0 \cdot 3$ for the larger. The values of the pitching moment calculated from the pressure distributions showed considerable scatter, but the phase lag in the moment was comparable to that obtained at a Mach number of $0 \cdot 4$ in the tests described in Ref. 1.

The Mach numbers of the German experiments are too low for a comparison to be made with the present results.

9. *Conclusions.*—For the values of the frequency parameter covered by the tests ($\omega < 0 \cdot 1$), it is found that no new features are introduced into the flow pattern by the oscillation of the aerofoil. There is, however, a phase difference between changes of the flow pattern and of the incidence of the aerofoil, and the pattern at a particular instantaneous incidence of the oscillation

---

* Such an oscillation occurs also[3] when the boundary layer is laminar on the surface of an aerofoil which is not oscillating ; it is associated with the interaction of shock-waves with the boundary layer.

† In the photographs taken with transition fixed a phase difference was visible in the shock-waves associated with the spoilers. Examination of all the photographs (including those reproduced in Fig. 13) showed that this difference was of the same order as that for the main shock-waves.

thus resembles that for steady motion at a different incidence. The phase difference could be determined most accurately from measurements of the positions of the regions, close to the surface of the aerofoil, where transition from laminar to turbulent flow occurred in the boundary layer. The phase differences derived in this way were found to be of the same order as those determined from observations of the shock-wave pattern and of the boundary-layer separation points, and are thus assumed to represent the phase difference of the flow pattern in general. In part of the work boundary-layer transition was fixed artificially close to the leading edge, and the analysis was then based on the positions of the shock-waves.

The experiment was made for two positions of the axis of oscillation ($0 \cdot 195c$ and $0 \cdot 445c$). For the rearward axis, direct measurements of the pitching-moment derivatives had been made in a previous experiment. A comparison is, therefore, possible between the phase difference of the flow pattern and the phase difference of the pitching moment calculated from the derivative measurements, and when allowance is made for the inherent inaccuracies of the present technique it is found that there is reasonable agreement over the range of Mach number covered ($0 \cdot 7 < M < 0 \cdot 9$). When the axis is moved forward to $0 \cdot 195c$ the phase difference of the flow pattern does not change greatly.

Calculations for a flat plate in incompressible flow show that the phase difference in the circulation is also in reasonable agreement with the phase difference in the pitching moment for the rearward axis, and does not change greatly when the axis is moved to its forward position. It is, therefore, concluded that the observed phase difference in the flow pattern corresponds to that in the circulation round the aerofoil. This conclusion is supported by some semi-empirical calculations made by W. P. Jones which again show good agreement between the phase differences in the circulation and pitching moment for the aerofoil when oscillating about the rearward axis position in a stream moving at high subsonic speeds.

Tests made with the axis at $0 \cdot 445c$ showed that the phase difference in the flow pattern is insensitive to amplitude for amplitudes up to 4 deg, and is approximately proportional to the frequency parameter ω.

Any phase difference that is present when the aerofoil is oscillating in a supersonic stream ($M = 1 \cdot 6$) is too small to be detected in photographs.

REFERENCES

No.	Author	Title, etc.
1	J. B. Bratt, W. G. Raymer and J. E. G. Townsend.	Measurements of pitching moment derivatives for two-dimensional models at subsonic and supersonic speeds, and for a rectangular model of aspect ratio 4 at subsonic speeds. (In preparation.)
2	H. H. Pearcey	The indication of boundary-layer transition on aerofoils in the N.P.L. 20-in. × 8-in. High Speed Wind Tunnel. C.P. 10. December, 1948.
3	D. W. Holder and R. J. North	An oscillatory flow resulting from the interaction of shock-waves with the boundary layer on a rigid aerofoil. A.R.C. 12,400. June, 1949. (To be published.)
4	E. T. Whitaker and G. Robinson	*The Calculus of Observations*, pp. 280 to 282. Blackie and Son, Ltd. London.

REFERENCES—*continued.*

5	H. Glauert	The force and moment on an oscillating aerofoil. R. & M. 1242. 1929.
6	W. P. Jones	Summary of formulae and notations used in two-dimensional derivative theory. R. & M. 1958. August, 1941.
7	W. P. Jones	Wind-tunnel wall interference effects on oscillating aerofoils in subsonic flow. R. & M. 2943. December, 1953.
8	J. B. Bratt and A. Chinneck	Measurements of mid-chord pitching-moment derivatives at high speeds. R. & M. 2680. June, 1947.
9	T. Zobel	Progress in optical measurements of flow. (FB 1934 and Schriften der Akademie der Lufo No. 5008/44.) Ministry of Supply R. & T. 327. GDC. 10/1429T. A.R.C. 11,643. January, 1947.
10	A. Ritter	Druckverteilungsmessungen an schwingenden flügeln mit der interferenzmethode. Ministry of Supply R. & T. 262. 1946.

LIST OF SYMBOLS

A	Coefficient of $\sin \phi$ in the least-squares analysis (*see* section 5)
B	,, ,, $\cos \phi$,, ,, ,, ,, (,, ,, ,,)
c	Aerofoil chord length
$E_{A,(B),(\varepsilon)}$	Probable error in the determined value of A, (B), (ε)
f	Frequency of oscillation of the aerofoil
M	Free-stream Mach number
M_0	Oscillatory pitching moment
M_θ	Coefficient of the in-phase component of M_0
$M_{\dot\theta}$	,, ,, ,, out-of-phase ,, ,, M_0
m_θ	Non-dimensional form of M_θ $(= M_\theta/\rho V^2 c^2)$
$m_{\dot\theta}$	,, ,, ,, $M_{\dot\theta}$ $(= M_{\dot\theta}/\rho V c^3)$
q	Probable error in measuring x_T/c
t	Time
V	Free-stream velocity
x_T	Distance of transition region from leading edge of aerofoil
α_0	Mean incidence of oscillation of the aerofoil
ε	Phase difference between movement of flow pattern and forcing motion
η	,, ,, ,, variation of pitching moment and forcing motion
θ	Instantaneous angle of incidence of the aerofoil
θ_0	Amplitude of oscillation of the aerofoil
ρ	Free-stream density
ϕ	Phase of forcing motion
ω	Frequency parameter

9

B
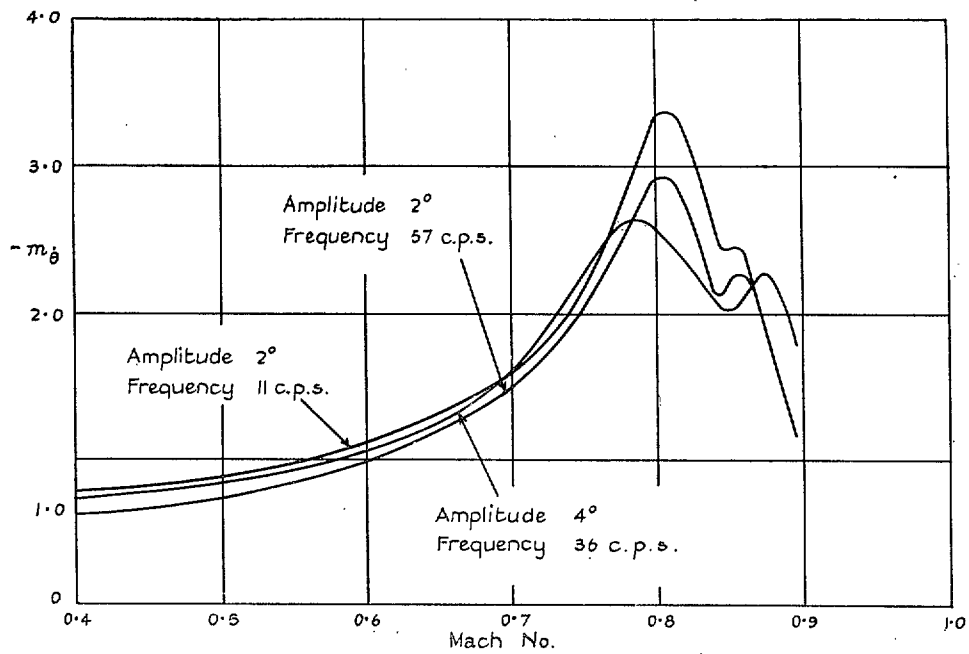
FIG. 1.   Variation of — $m_{\dot\theta}$ with Mach number at zero mean incidence (from Ref. 1).
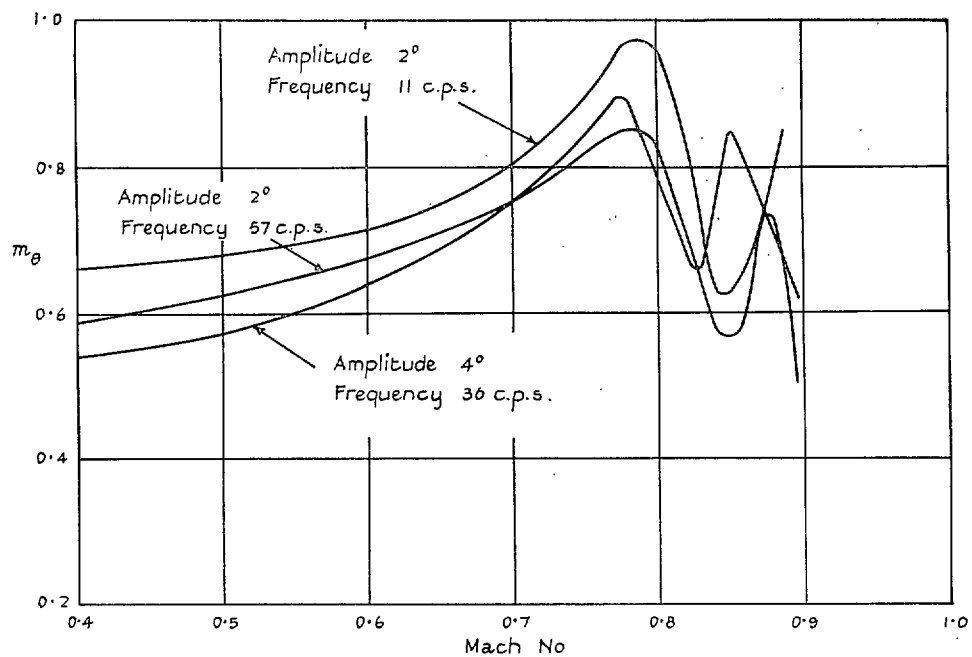

FIG. 2.   Variation of m_θ with Mach number at zero mean incidence (from Ref. 1).
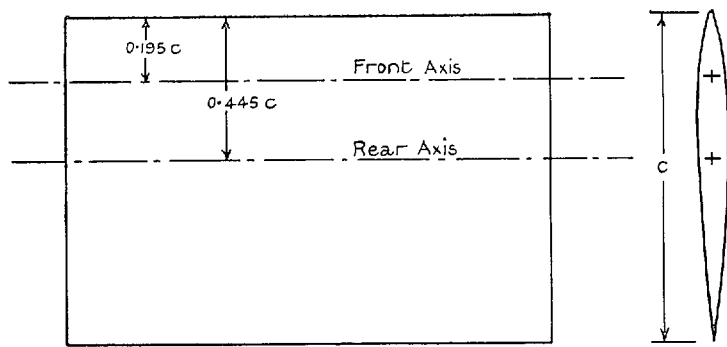
10

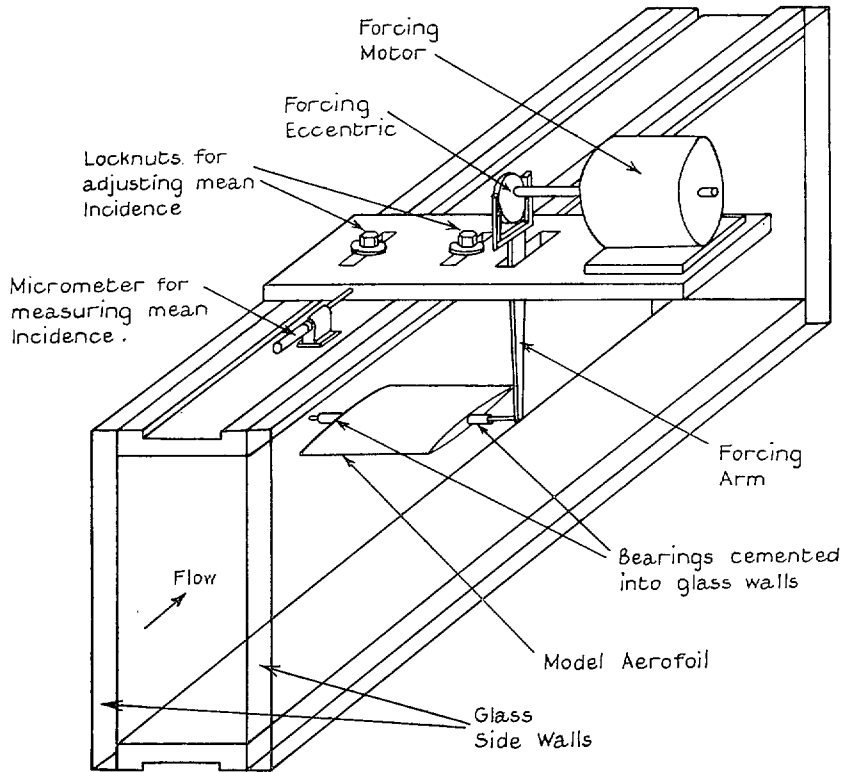FIG. 3.   Details of the model aerofoils.

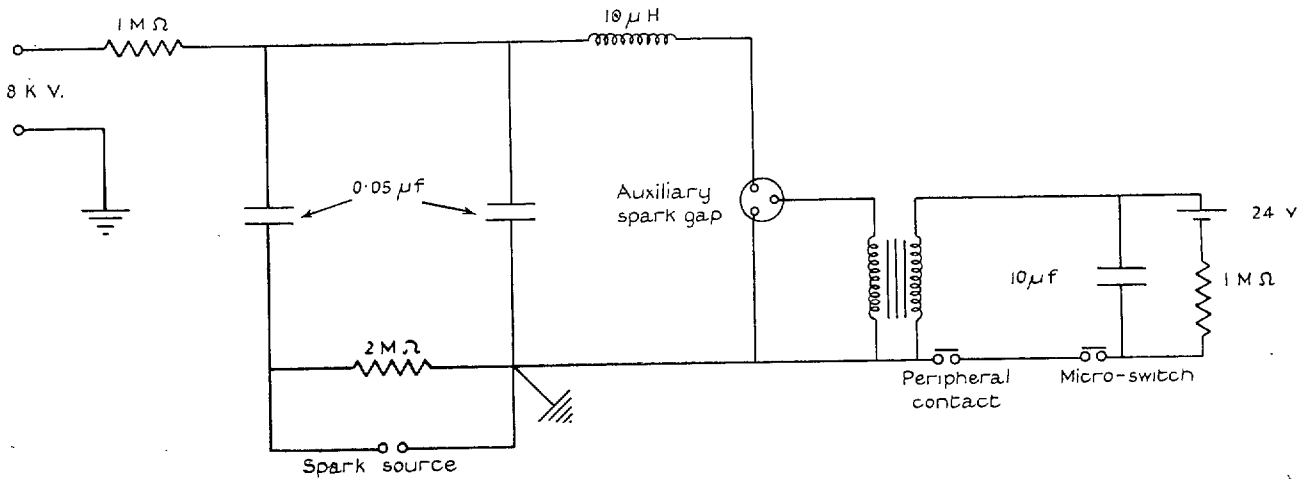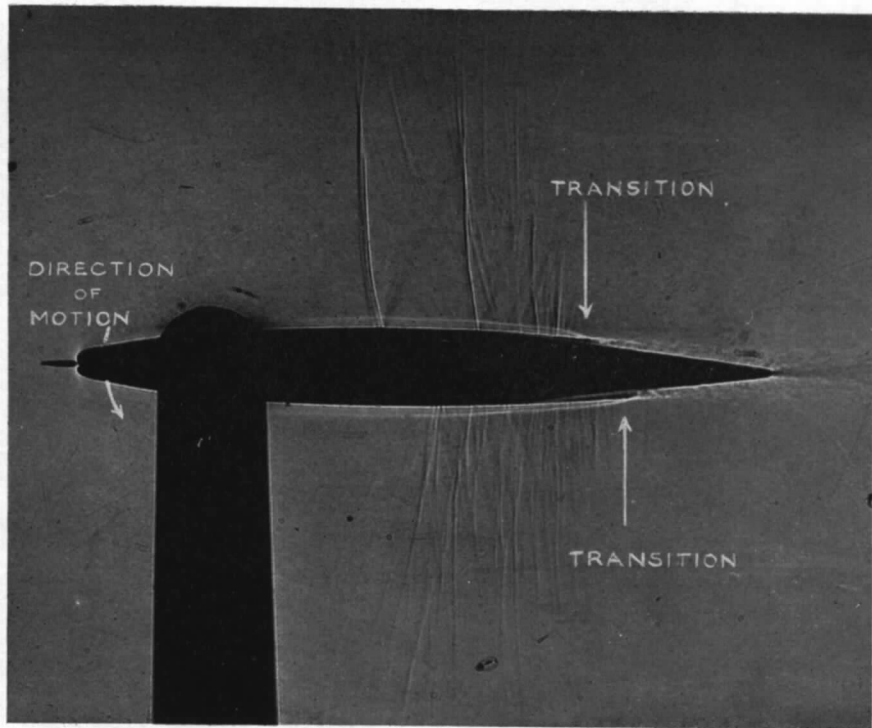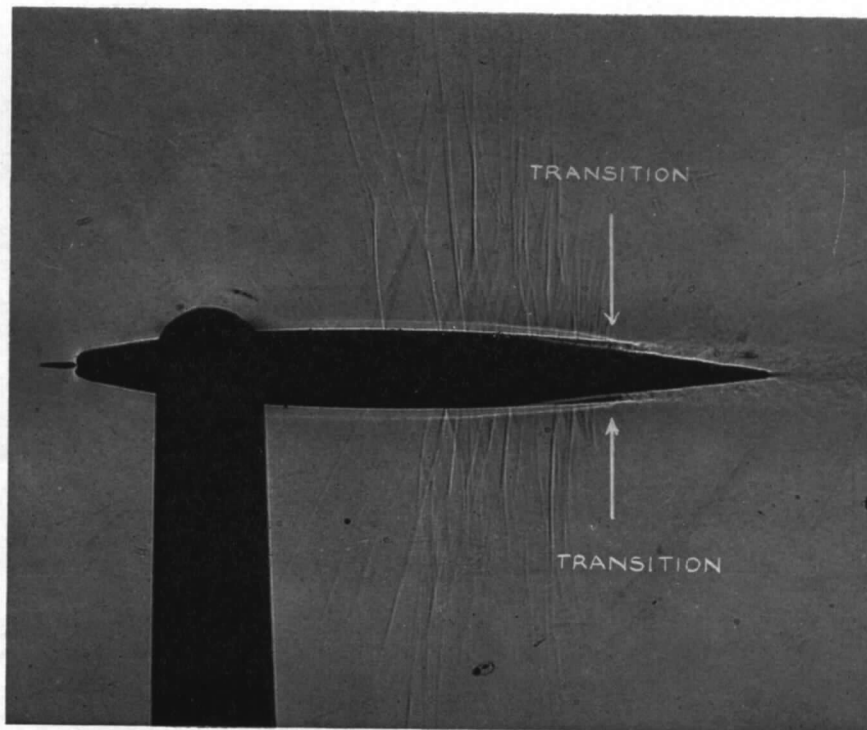
FIG. 4.   Sketch of the forcing apparatus.

FIG. 5.   Diagram of the final trigger circuit.

11

Oscillatory 60 c.p.s.

Static

FIG. 6.   Photographs of the aerofoil at zero incidence showing the transition regions and the differences between the static and oscillatory cases.
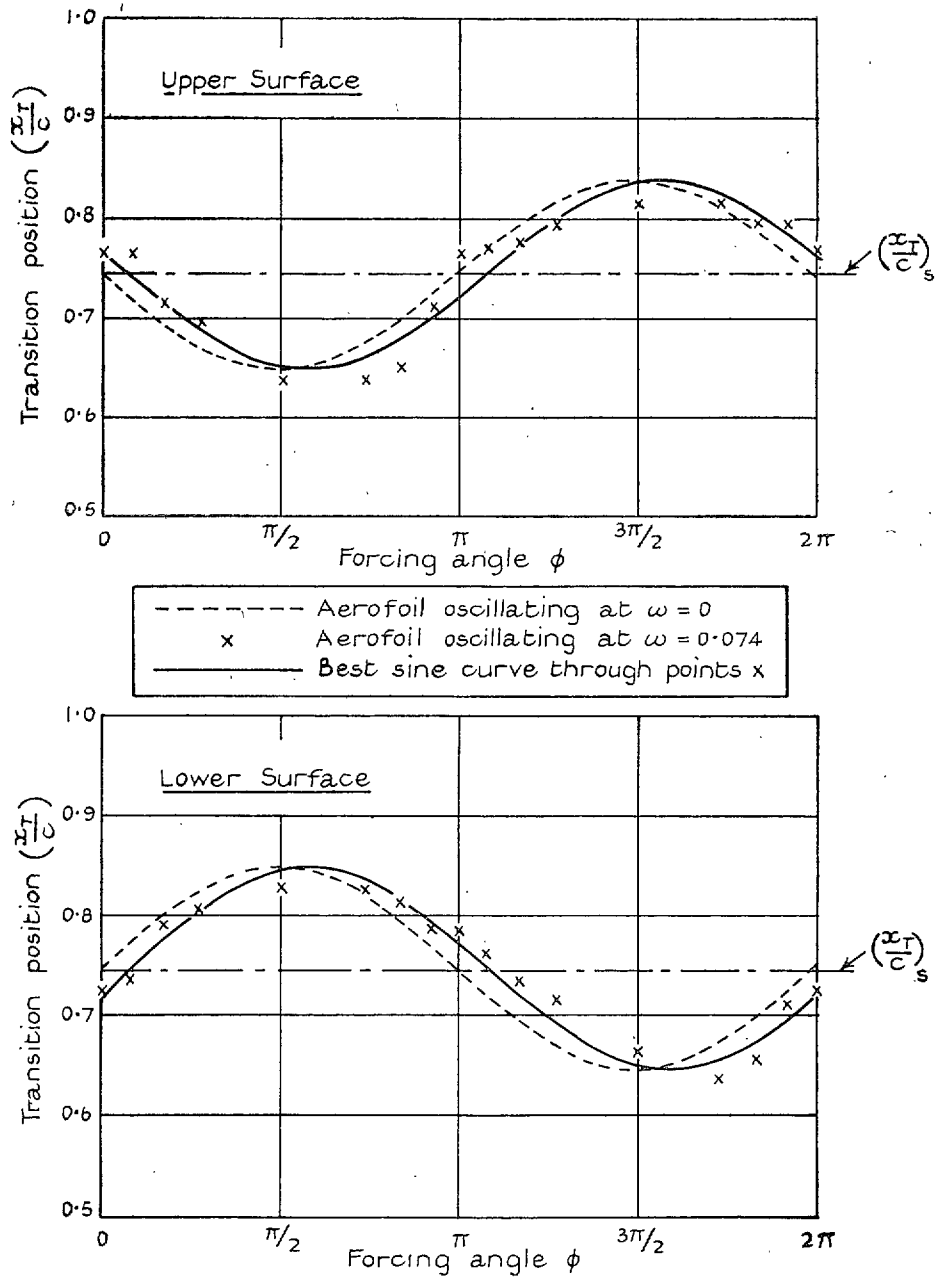
FIG. 7. Typical measurements of the movement of the transition regions in a cycle. $\alpha_0 = 0$ deg. $\theta_0 = 2$ deg. Axis at $0\cdot445c$. $M = 0\cdot82$.

13
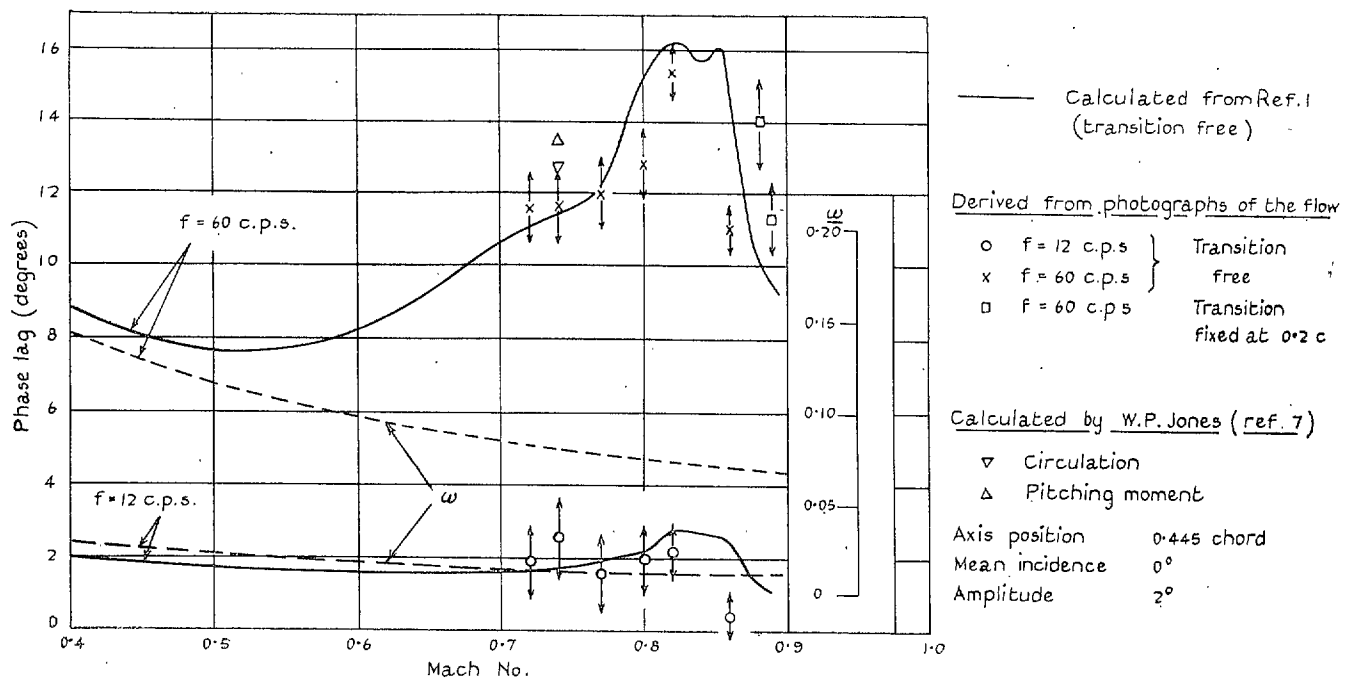
FIG. 8. Variation of phase lag with Mach number for two frequencies.
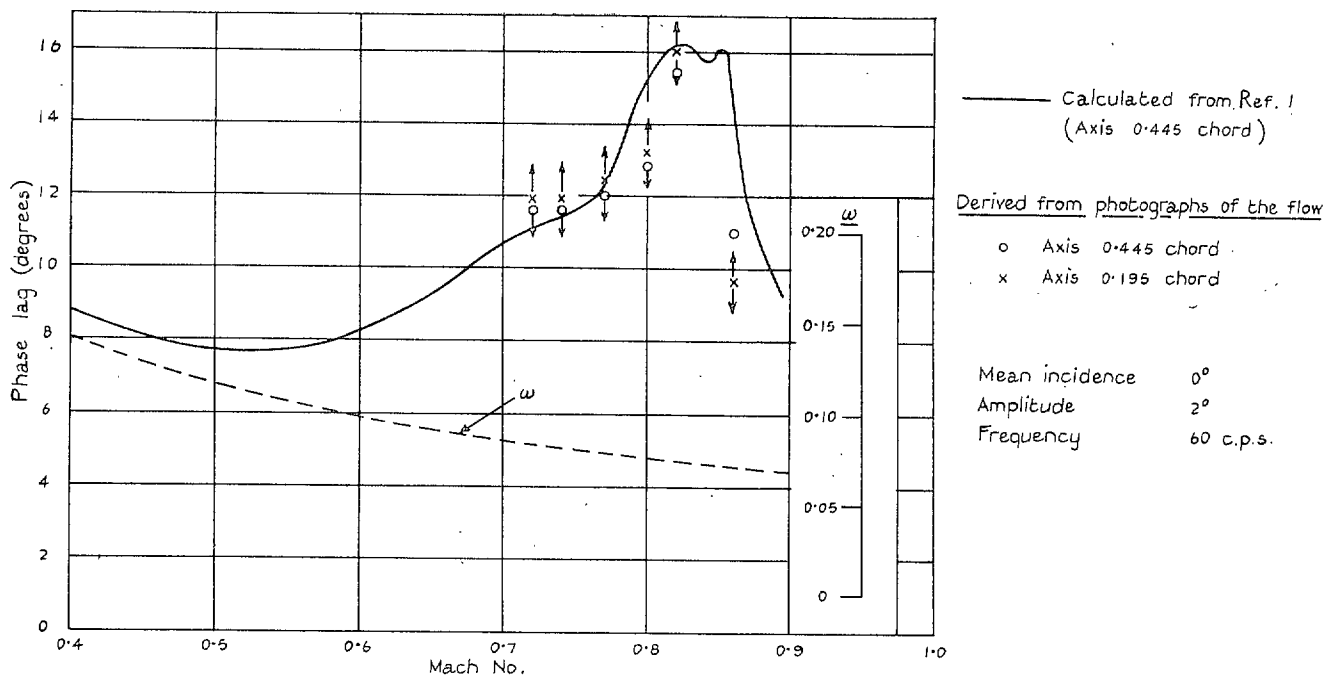
FIG. 9. Variation of phase lag with Mach number for two positions of the axis of oscillation.

14
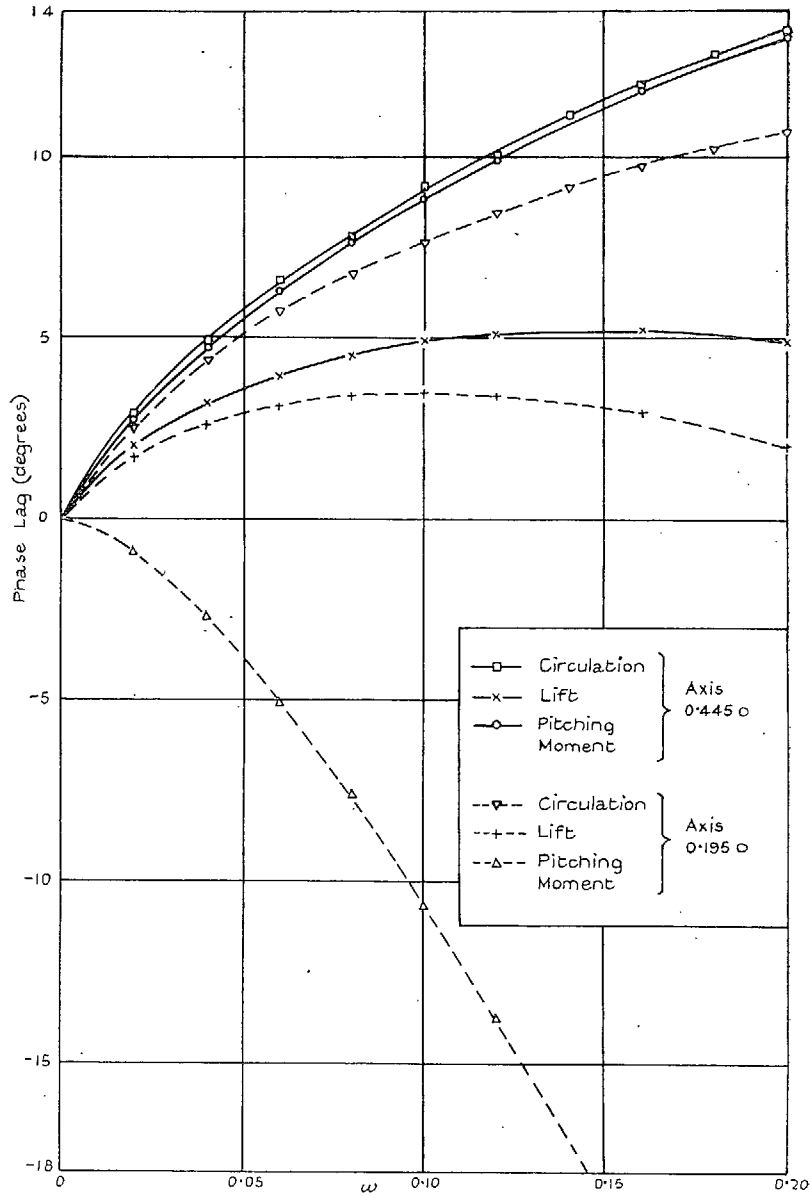
FIG. 10.   Variation of phase lag with the frequency parameter calculated
for a flat plate in incompressible flow.
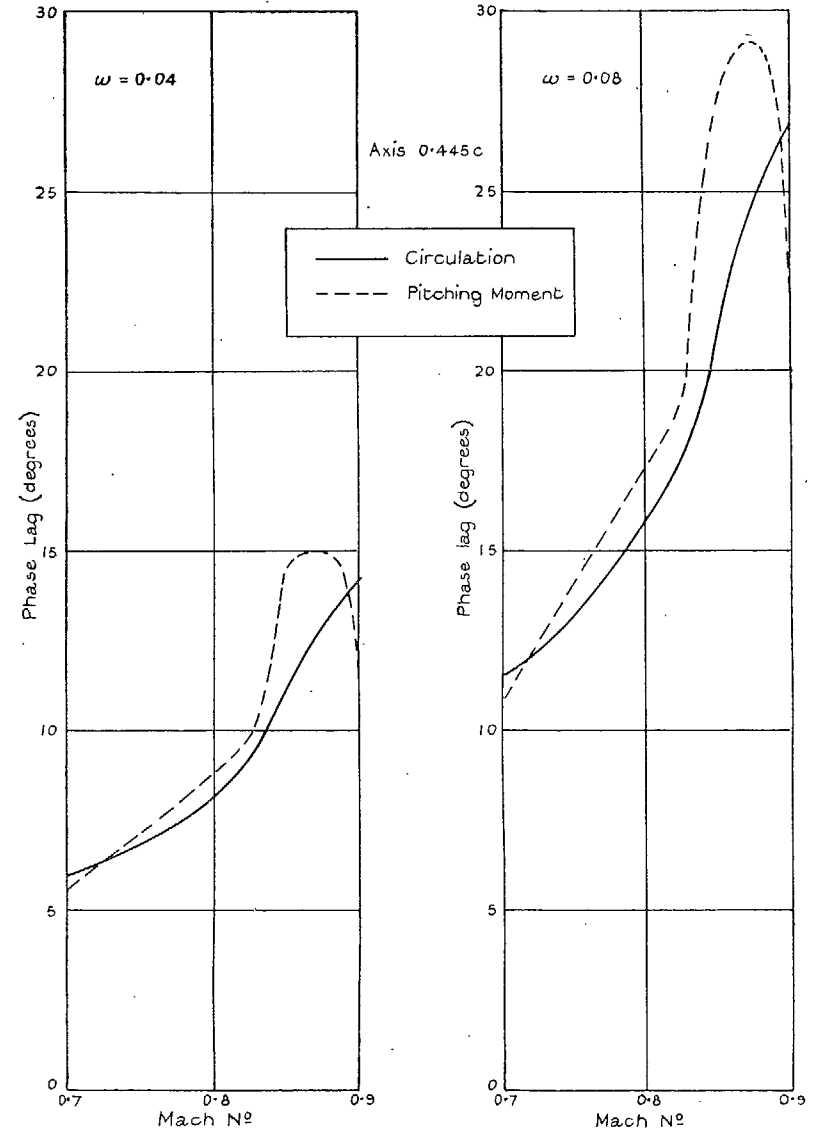
FIG. 11.   Calculated phase lag for two values of the frequency
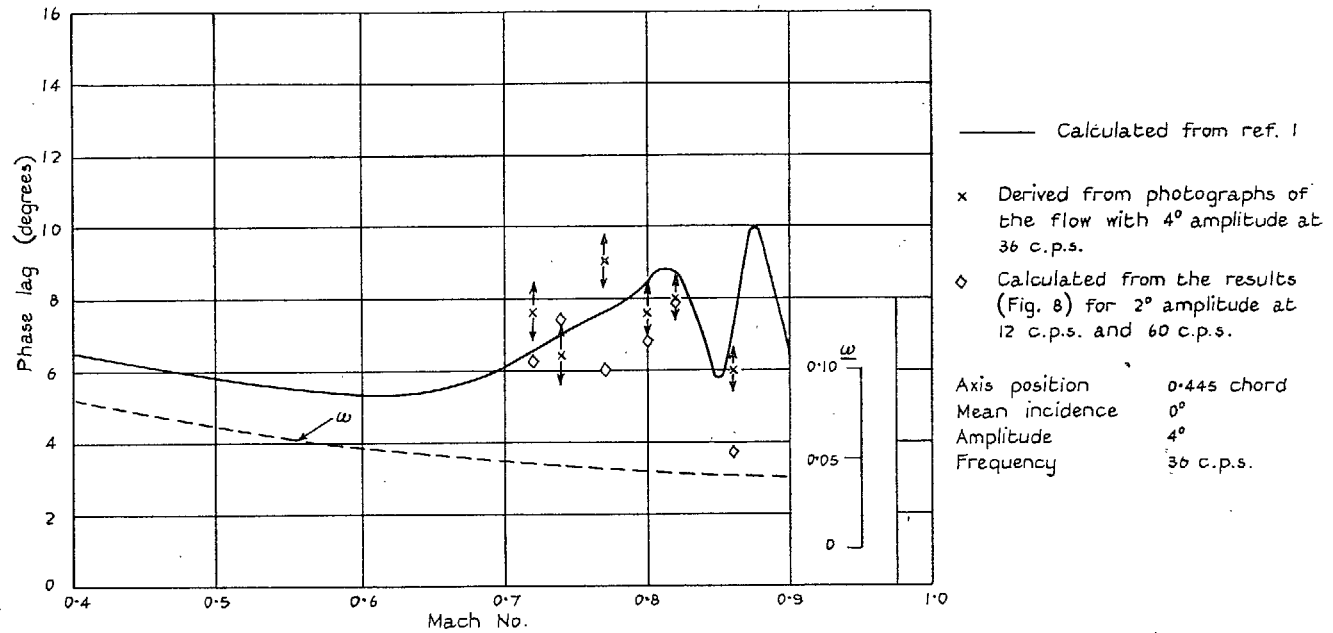parameter (Ref. 7).

FIG. 12.   Variation of phase lag with Mach number for large amplitude.
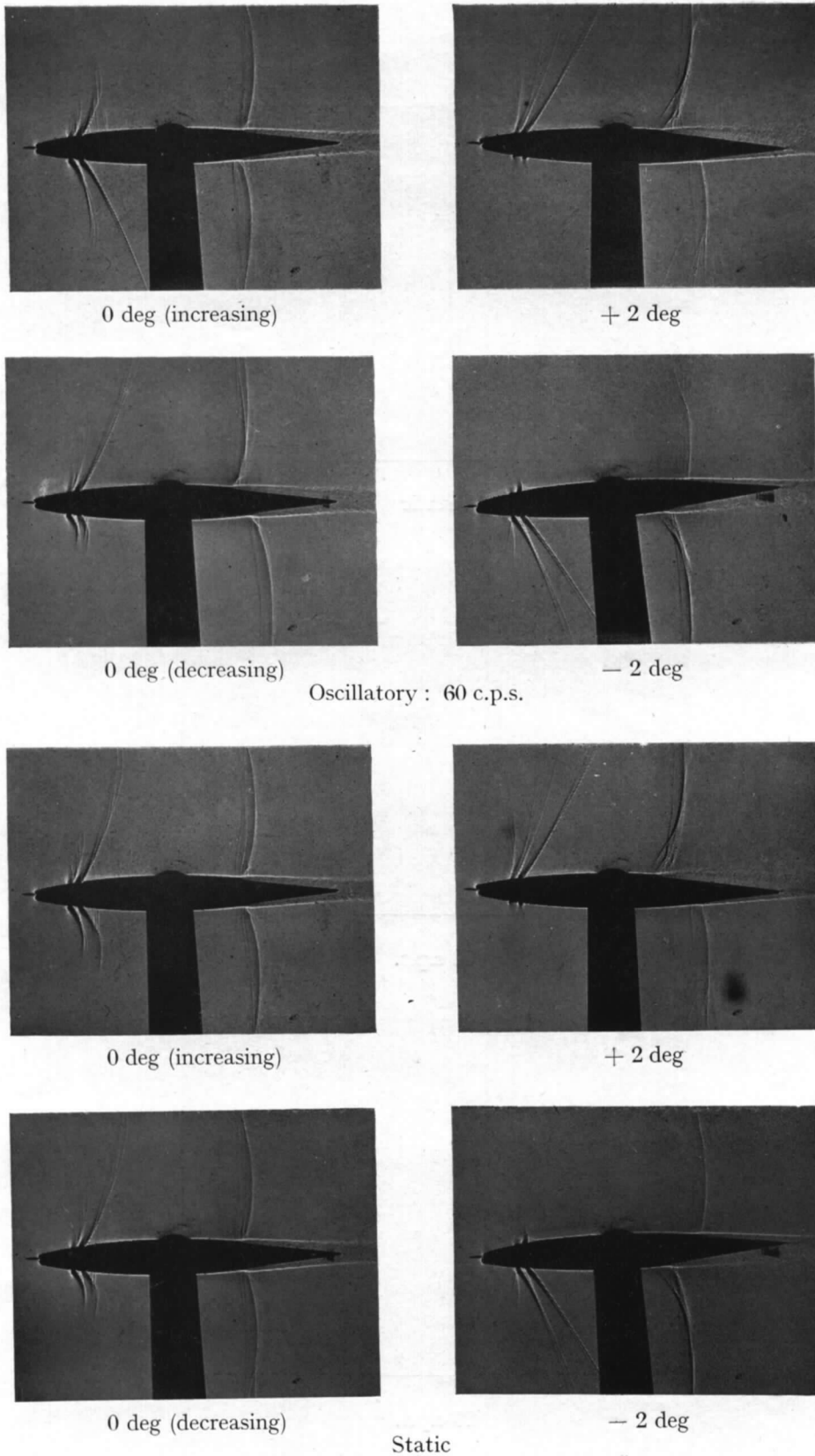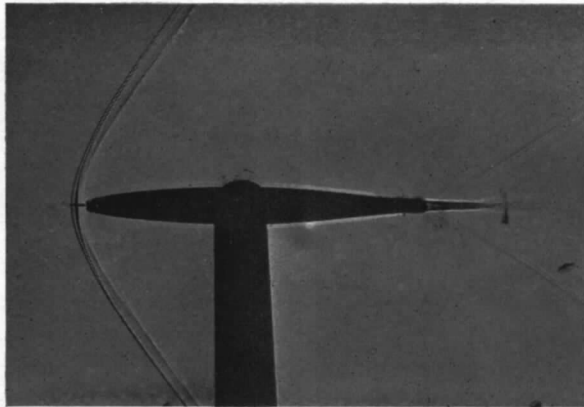
0 deg (increasing)   + 2 deg

0 deg (decreasing)   − 2 deg

Oscillatory : 60 c.p.s.

0 deg (increasing)   + 2 deg

0 deg (decreasing)   − 2 deg

Static
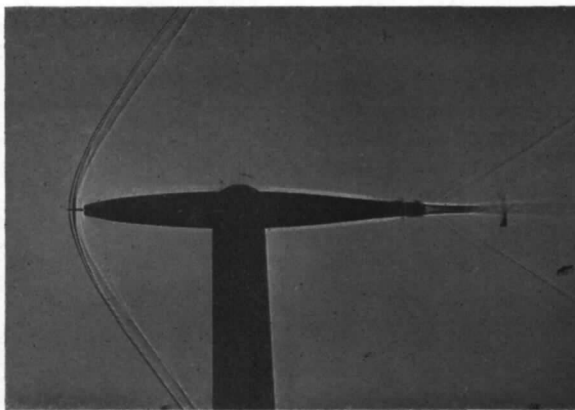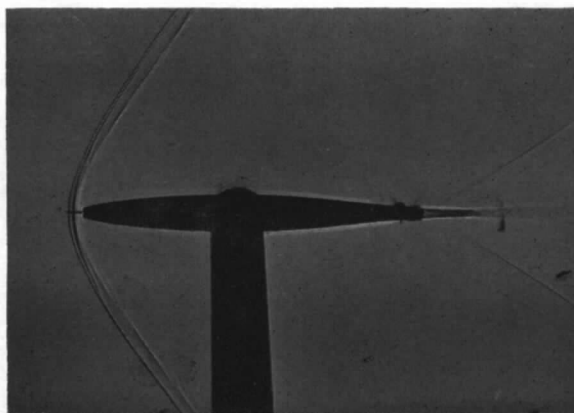
FIG. 13.   Photographs of the flow around the aerofoil with its axis 0·445 chord.
$M = 0·88$ (transition fixed).   Mean incidence 0 deg ; amplitude 2 deg.

17

Static

30 c.p.s.

60 c.p.s.

FIG. 14.   Photographs at $M = 1 \cdot 60$.

Publications of the Aeronautical Research Council

ANNUAL TECHNICAL REPORTS OF THE AERONAUTICAL RESEARCH COUNCIL (BOUND VOLUMES)

1936 Vol. I. Aerodynamics General, Performance, Airscrews, Flutter and Spinning. 40s. (41s. 1d).

Vol. II. Stability and Control, Structures, Seaplanes, Engines, etc. 50s. (51s. 1d.)

1937 Vol. I. Aerodynamics General, Performance, Airscrews, Flutter and Spinning. 40s. (41s. 1d.)

Vol. II. Stability and Control, Structures, Seaplanes, Engines, etc. 60s. (61s. 1d.)

1938 Vol. I. Aerodynamics General, Performance, Airscrews. 50s. (51s. 1d.)

Vol. II. Stability and Control, Flutter, Structures, Seaplanes, Wind Tunnels, Materials. 30s. (31s. 1d.)

1939 Vol. I. Aerodynamics General, Performance, Airscrews, Engines. 50s. (51s. 1d.)

Vol. II. Stability and Control, Flutter and Vibration, Instruments, Structures, Seaplanes, etc. 63s. (64s. 2d.)

1940 Aero and Hydrodynamics, Aerofoils, Airscrews, Engines, Flutter, Icing, Stability and Control, Structures, and a miscellaneous section. 50s. (51s. 1d.)

1941 Aero and Hydrodynamics, Aerofoils, Airscrews, Engines, Flutter, Stability and Control, Structures. 63s. (64s. 2d.)

1942 Vol. I. Aero and Hydrodynamics, Aerofoils, Airscrews, Engines. 75s. (76s. 3d.)

Vol. II. Noise, Parachutes, Stability and Control, Structures, Vibration, Wind Tunnels. 47s. 6d. (48s. 7d.)

1943 Vol. I. Aerodynamics, Aerofoils, Airscrews, 80s. (81s. 4d.)

Vol. II. Engines, Flutter, Materials, Parachutes, Performance, Stability and Control, Structures. 90s. (91s. 6d.)

1944 Vol. I. Aero and Hydrodynamics, Aerofoils, Aircraft, Airscrews, Controls. 84s. (85s. 8d.)

Vol. II. Flutter and Vibration, Materials, Miscellaneous, Navigation, Parachutes, Performance, Plates, and Panels, Stability, Structures, Test Equipment, Wind Tunnels. 84s. (85s. 8d.)

ANNUAL REPORTS OF THE AERONAUTICAL RESEARCH COUNCIL—

1933–34	1s. 6d. (1s. 8d.)	1937	2s. (2s. 2d.)
1934–35	1s. 6d. (1s. 8d.)	1938	1s. 6d. (1s. 8d.)
April 1, 1935 to Dec. 31, 1936.	4s. (4s. 4d.)	1939–48	3s. (3s. 2d.)

INDEX TO ALL REPORTS AND MEMORANDA PUBLISHED IN THE ANNUAL TECHNICAL REPORTS, AND SEPARATELY—

April, 1950 – – – – R. & M. No. 2600. 2s. 6d. (2s. 7½d.)

AUTHOR INDEX TO ALL REPORTS AND MEMORANDA OF THE AERONAUTICAL RESEARCH COUNCIL—

1909–1949 – – – – – R. & M. No. 2570. 15s. (15s. 3d.)

INDEXES TO THE TECHNICAL REPORTS OF THE AERONAUTICAL RESEARCH COUNCIL—

December 1, 1936 — June 30, 1939.	R. & M. No. 1850.	1s. 3d. (1s. 4½d.)
July 1, 1939 — June 30, 1945.	R. & M. No. 1950.	1s. (1s. 1½d.)
July 1, 1945 — June 30, 1946.	R. & M. No. 2050.	1s. (1s. 1½d.)
July 1, 1946 — December 31, 1946.	R. & M. No. 2150.	1s. 3d. (1s. 4½d.)
January 1, 1947 — June 30, 1947.	R. & M. No. 2250.	1s. 3d. (1s. 4½d.)
July, 1951 – – – –	R. & M. No. 2350.	1s. 9d. (1s. 10½d.)

Prices in brackets include postage.

Obtainable from

HER MAJESTY'S STATIONERY OFFICE